RADOME RAIN EROSION TESTING

BY MEANS OF SUPERSONIC SLEDS

M/R 16-875 May 1956

Prepared by

RAYTHEON MANUFACTURING COMPANY
MISSILE SYSTEMS DIVISION

Bedford, Massachusetts

for

THE OHIO STATE UNIVERSITY

WRIGHT AIR DEVELOPMENT CENTER
RADOME SYMPOSIUM

Columbus, Ohio
June 4, 5, and 6, 1956

Prepared by:

Chester L. Smith

Chester L. Smith

ABSTRACT

A method is presented of determining the sled travel in a known artificial rain field required to obtain the same erosion damage (if any) encountered by a missile in free flight in any given natural rain. The conditions of test and the mathematics of simulation are discussed. Methods used to determine the "worst case" of erosion, which is used to determine the maximum sled travel, are shown, and methods of rain field sampling to obtain droplet size, distribution, and rainfall rate are given.

1. INTRODUCTION

The severe damage sometimes suffered by flying in weather conditions where the air is full of particles poses a problem in the design of any moving vehicle. Three types of airborne particles are known to cause damage, (1) rain, (2) hail and (3) sand. This discussion will be confined to the case of rain except for some general comments on the relative importance of the other two particle classes.

In order to obtain specific information about the relative rain erosion resistance of various radome materials three main attacks on the problem have been made by various laboratories: (1) Whirling Arm [2,6] (2) Flight in natural rain [6] and (3) Ballistic test in spray field. [2] The whirling arm technique, as it is currently performed, is good subsonically. The flight through natural rainfall by an aircraft carrying samples is a dangerous operation and the results, while demonstrating the existence of erosion, are not quantitative, since radar studies have shown natural rains to be non-homogeneous. The ballistic method is good for supersonic uses, provided that a correlation between natural rains and the spray field can be given. The small size of the test specimen and the few impacts made with droplets in this method make an interpretation of the integrated effect very difficult.

A fourth method, pioneered by Dittmann [2] and others at Convair is the supersonic sled. A full size article, say a radome, is mounted on a rocket propelled sled similar to those used for other captive high speed tests and fired through a spray field at a speed near Mach 2. The problem is to correlate the sled test with an equivalent natural rainfall. Since neither the particle distribution in the spray field nor the time velocity history of the sled run are precisely the same as the quantities of a free firing in natural rain, some means of relating them must be found in order to interpret the results.

2. METHOD OF TEST

2.1 The Sled

The test vehicle is a two-unit sled arranged as shown in Figure 1. The purpose of the two-unit sled instead of one large one is that it behaves very much like a two stage rocket. By keeping the frontal area of the booster unit the same as the main sled the drag is essentially the same as a single sled. Both units carry seven JATO motors and shortly after a speed of Mach 1 (booster burnout) is reached, the booster disconnects. The main sled now fires and accelerates to a speed in the vicinity of Mach 2.0 which is maintained until the spray field has been passed. A water brake is used to stop the main sled. Aerodynamic drag, coupled with a lower velocity, is expected to slow the booster before it reaches the water. It is equipped with a water brake scoop to bring it to a full stop short of the main sled.

2.2 The Spray Field

The spray field occupies the 2100 feet of track where the sled speed is maximum.

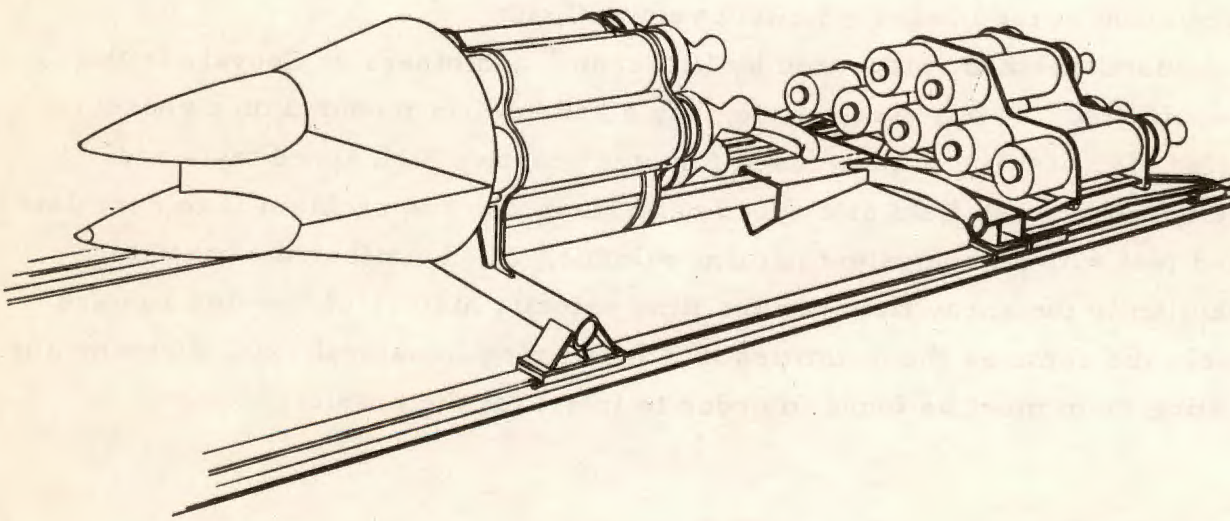

Figure 1 - Test Sled and Booster Combination

The nozzles used are the Spraying System (O. (Chicago, Ill.) Vee Jet 1/4 U 8050. Since the erosion effect is proportional to some positive power greater than unity of the particle diameter, the more-erosive larger droplets make possible some saving in the number of sled runs needed in any given simulated rain rate. The highest equivalent rain fall rate (5 in. /hr) is obtained with a pressure of 4.5 psig and a symmetrical separation of 18 feet. Nozzles are directed upwards 50°, and are located six feet apart along the length of the spray field in pairs as indicated in Figure 2.

2.3 Drop Size Distribution

The method of measuring the distribution of water throughout the range of drop size consisted of capturing the drops in oil pans and measuring them visually. First the drops were captured in an oil pan which had two kinds of oil in it, see Figure 3.

The two kinds of oil do not mix readily so the drops which fell into the motor oil descended slowly and rested on top of the silicon oil. The captured

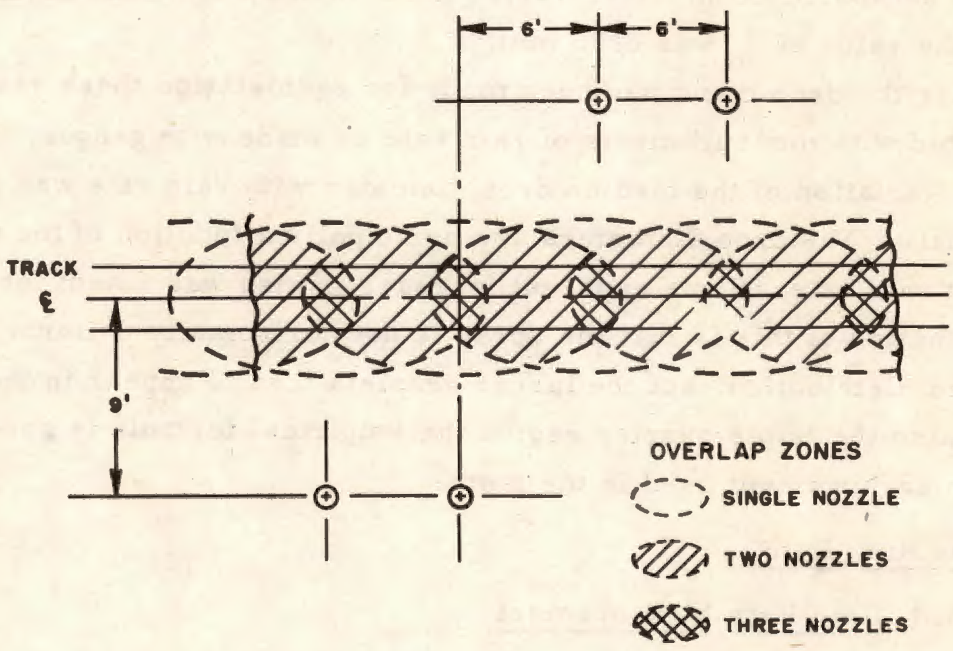

Figure 2 - Spray Nozzle Deployment

Figure 3 - Oil Pan Detail

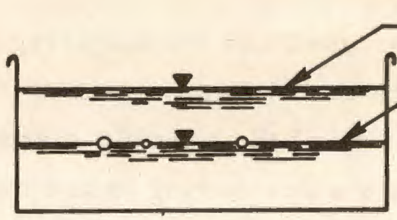

drops were then photographed 1:1. The droplets can be preserved for several days before the oils begin to mix or appreciable water absorption takes place. The photos were made immediately after droplet capture. Comparison with photographs of drops in air showed that the shape was not distorted sufficiently to cause appreciable error.

Reading the negatives was performed by measuring each droplet with a comparator. This method proved to be tedious. While a scanning counter exists the negatives were not suitable for its use. It was found that certain persons could, after some practice, estimate the drops in each group very accurately. In a trial of this method one girl was able to reduce the time required to read a photograph from 5 hours (two people) to 24 minutes (two people). The estimated count never varied more than 1% from the actual and the error in the value of d_o was 0.03 mm.

After the drop count had been made for each station these readings were correlated with measurements of rain rate as made with gauges. It was found that the variation of the median drop diameter with rain rate was comparatively small. The drop diameters are principally a function of the nozzle pressure, not rain rate. Some apparent increase in size was noted: however, the best explanation of this is that the spray is not horizontally uniform with respect to size distribution, but the larger droplets tend to appear in the edges. Since this is also the triple overlap region the empirical formula is good only for the nozzle arrangement used in the tests.

2.4 The Rain Rate

2.4.1 Rain Rate Measurement

A system of rain gauges similar to that shown in Figure 4 were used to measure the rain rate. Several determinations were made for each set of field conditions and the results averaged.

Figure 4 - Rain Gauge

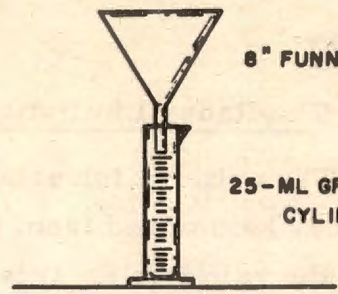

Measurements made with a row of gauges spaced 18 inches apart down the field at the anticipated center line of the radome showed the rain not only to be heavy at all stations but also to have a high variation. The range of rates for the spacing and arrangement shown in Figure 2 was 3.82 to 8.68 inches per hour. The rms value of I was 5.05 in./hr. The correlation of I with d_o was found to be:

$$*d_o = 1.56\, I^{.145}$$

where d_o is in. mm

I is rain rate in./hr

The small value of the exponent of I indicates that drop size growth with increasing rain rate is small. In natural rainfall the corresponding exponent is in the neighborhood of 0.20 to 0.30 with a few observers [1] reporting numbers up to 0.37 and 0.40.

$*d_o$ = the drop diameter which divides the amount of water into two equal portions.

3. THEORY

3.1 The Radar Limitation

The criteria for establishing the equivalent rainfall conditions in the tests may be derived from the limitations imposed upon the radar guidance system by the rain itself. It is obvious that some rainfalls which have a finite probability of occurring, can be sufficiently severe as to completely neutralize any weapon system that depends upon electromagnetic radiation in the microwave region or higher.

The range to lock-on is given by:

$$R = C \left[\frac{\sigma P \lambda^2 G_1(\phi, \theta) G_2(\phi, \theta)}{L^2} \right]^{1/4} \qquad (1)$$

where C = constant relating to system of measurement (i.e. km, stat. mi., naut. mi., etc.)

P = Power transmitted

σ = radar cross-section of target

λ = wavelength

$G(\phi, \theta)$ = The gain function antenna system

L = Path loss

The path L is governed by the maximum allowable two-way path attenuation which will permit a reliable lock-on. If this is assumed to be 3 db above the ambient noise level, then R_{LO} can be determined for given values of the other variables.

Where scattering or absorptive particles are present in the volume between the radar and the target, the lock-on range is reduced to the point where the signal returned is detectable 3 db above the ambient noise level. The formula:

$$\alpha = \frac{10\, I}{\lambda^2 L} \qquad (2)$$

where I = rain rate in. /hr

λ = wavelength

L = path length mi

α = db/mile

yields satisfactory results for values of I up to about one inch per hour. Above that point the results are likely too low.

Where pulse radars are used, back scattering may be a serious problem. The scattered energy between the radar and the target acts as a noise generator on the radar frequency. Time gated radars are naturally sensitive to this return.

The Doppler spectrum returned from a moving group of particles to a moving observer is:

$$\psi_R = \sum n_i \left(\bar{u} \cdot \bar{V}_m + \sum \bar{u} \cdot \bar{V}_i\right) \tag{3}$$

when: n_i is the wave numbers of the transmitted frequencies.

$\bar{u}$ = unit vector along line of sight.

$\bar{V}_m$ = velocity of moving observer.

$\bar{V}_i$ = velocity of droplets in i^{th} group.

The presence of a discrete target within the field introduces another term in equation of the form

$$\psi_T = \sum n_i \left(\bar{u} \cdot \bar{V}_m + \bar{u} \cdot \bar{V}_T\right) \tag{4}$$

$\bar{V}_T$ is the velocity of the target.

$$\text{If: } \bar{u} \cdot \bar{V}_T = r \; \bar{u} \cdot \bar{V}_m \tag{5}$$

then combining 3, 4, & 5

$$\psi = \sum n_i \left[\bar{u} \cdot \bar{V}_m \; (1 + r) + \sum \bar{u} \cdot \bar{V}_i\right] \tag{6}$$

The Doppler frequencies of the target appear as a group separated from the continuum $n_i \left(\bar{u} \cdot \bar{V}_m + \sum_m \bar{u} \cdot \bar{V}_i\right)$

if $r > r_m$

where r_m is the velocity ratio of the moving observer to the fastest moving drop group (mth group). In a practical system (i. e. the moving observer* is a missile emitting a single frequency of wave number n) the Doppler return may be filtered by a high pass device such that

*It is a matter of indifference whether the missile is actually transmitting or not if the illuminator can satisfy the conditions required.

$$f_m < \dot{\psi}_p < f_T \;. \tag{7}$$

The remaining factor is the attenuation caused by absorption and scattering. The attenuation effect for $\lambda = 3$ cm is shown in Figure 5.

Where the relative velocity of target and radar is zero, the Doppler frequency drops to zero and both effects must be considered. A condition such as this occurs if the target orbits around the radar location, or if the target and airborne radar move at the same velocity, as in a tail chase.

3.2 Erosion Factor

It has been shown by Marshall and Palmer [4] that the drop size distribution of most natural rainfalls can be represented by

$$N = N_o e^{-\Lambda d} \tag{8}$$

where N = number of drops in group $d + \delta d$

N_o = number of drops in group $d = 0$

Λ = function of the rain rate I.

Treating Λ as a constant (i.e. I = constant)

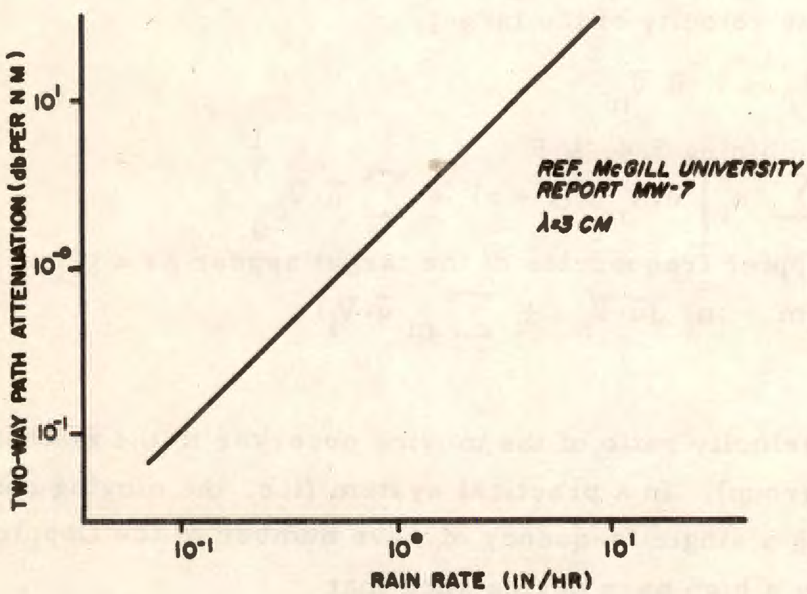

Figure 5 - Attenuation vs Rain Rate

The inpact stress is proportional to the square root of the mass

$$p = \sqrt{m} = cd^{3/2} \quad (9)$$

Experimental results to date indicate that Equation 9 probably holds, or at least that the exponent 3/2 is a first approximation. Letting the exponent be k for purposes of theory, the erosion caused by the i^{th} group is:

$$E_i = N_i d_i^{\,k} \quad (10)$$

With the definitions given in equation 8 the total erosion factor (E_I) due to droplet size distribution is:

$$E_I = \int_0^\infty N d^k \, \delta d^k$$
$$= N_o \int_0^\infty e^{-\Lambda d} \, \delta d \quad (11)$$

which is readily integrated as:

$$E_I = \frac{N_o \Gamma(k+1)}{\Lambda^{k+1}} \quad (12)$$

That the erosion rate goes up enormously with increasing velocity has been established in sample tests by the Cornell Aeronautical Laboratory,[6] Convair[2] and others

$$R_E \propto V^b \quad (13)$$

The value of b has been determined from data published by Convair and is found to range between 3.5 and 8 for supposedly identical rain conditions. Probably the variation could be accounted for in the sizes of particles encountered. Let b be a constant and,

$$R_E = KV^b \quad (14)$$

The component of V effective in erosion is normal to the radome surface. From Figure 6 it can be seen that

$$R_E = KV_N^b = KV^b \cos^b \theta \quad (15)$$

The appearance of K is incidental in this discussion since we are concerned with the relative erosive abilities of two different drop distributions. The constant K may be omitted since it is divided out later in the analysis.

It has been shown by Atlas[1] that

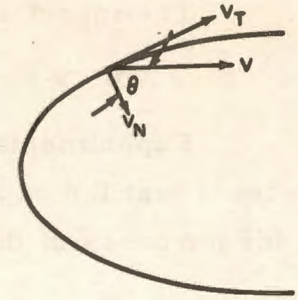

Figure 6 - Effect of Angle of Incidence on Rain Erosion

$$\Lambda = 3.75\, d_o \qquad (16)$$

and that d_o is related to rain intensity by:

$$d_o = 1.79\, I^{0.21} \quad \text{where I is in in. /hr} \qquad (17)$$

and d_o in. mm

The value of N_o in the Marshall and Palmer treatment is invarient with rain rate. While this may be a justifiable simplification for meterological purposes, closer examination of the data used shows that their equation fails to describe the numbers of smaller drops present. This is no criticism of the meterologists because they themselves point out this limitation. The difficulty comes in trying to correlate artificial rains where the drop distribution is quite different.

Both natural rainfall and artificial rain field droplet distribution can be described by:

$$N = e^{-\sum_{n=o}^{\infty} a_n d^n} = \prod_{n=o}^{\infty} e^{-a_n d^n} \qquad (18)$$

The erosion integral, in general terms, is:

$$E_I = \int_o^{\infty} \prod_{n=o}^{\infty} e^{-a_n d^n}\, d^k \quad dd \qquad (19)$$

unless K is a positive integer or zero the form is not readily integrated. However for practical purposes where N vs d has been experimentally found, the value of E_I may be obtained graphically by:

$$E_I \approx \sum N_i d_i^k \qquad (20)$$

At the stagnation point $\theta = 0$ and $R_E = K_7 V^b$ and the impact is less everywhere else. It has been shown by Wetterborg et al that aerodynamic considerations reduce the value of V_N below that given by equation 15. However, at the higher velocities the effect is less important and, considering the inexact state of rain erosion knowledge, probably can be neglected until some of the grosser aspects of the problem have been examined in more detail. Aerodynamics may affect the results if the velocity ratio between the sled speed and the free flight condition is not close to unity.

3.3 The Sled Simulation

The total erosion experienced by a radome traveling at a speed, V, through a rainfall, I, in a period of time, $t_2 - t_1$, is given by:

$$E = K \left[\int_{t_1}^{t_2} V_N^b \, dt \right] \int_0^{\infty} e^{-\sum_{n=o}^{\infty} a_n d^n} d^k \, dd \qquad (21)$$

The equation holds equally whether the radome is mounted on a free flying vehicle, or on a captive one like a sled. The object of the tests is to establish a valid estimate of the damage caused by certain natural rainfall. With this in view, it is necessary only to write a ratio between the natural and artificial erosion integrals.

$$\nu = \frac{K_m \int_{\text{missile}}^{\Delta t} V_N^b \, dt \int_o^{\infty} \left(\prod_{n=o}^{n=\infty} e^{-a_n d^n} \right) d^k \, dd \ \text{(Nat. Rain)}}{K_s \int_{\text{Sled}}^{\Delta t} V_N^b \, dt \int_o^{\infty} \left(\prod_{n=o}^{\infty} e^{-a_n d^n} \right) d^k \, dd \ \text{(Art. Rain)}} \qquad (22)$$

ν = number of sled runs required to simulate any given missile flight situation.

Since the material object is identical in both cases and the aerodynamics are similar if the speeds are nearly the same then:

$$K_m \approx K_s$$

and letting the velocity factor be denoted by E_v.

equation 22 becomes:

$$\nu = \frac{E_v \, E_I \text{ (Missile)}}{E_v \, E_I \text{ (Sled)}} \qquad (23)$$

The existence of a maximum ν depends on the flight history of the missile and upon the foreshortening of its range by rainfall intensity. Except where the limitation is severe the curve of V vs I is fairly constant after the maximum has been passed. The radar limitation is the stronger variable and the product of the two integrals tends to be nearly constant, or even to diminish despite the fact the rain intensity is increasing rapidly.

4. OTHER EROSION PROBLEMS

4.1 Snow Erosion

The apparent absence of snow erosion is evidently due to the small size of the erosive particle. While snow flakes may be quite large they consist of an airy lattice of individual crystals. Impact with such a structure would first collapse the lattice and then demolish the crystals. Current aircraft and missiles are not significantly affected, but when the relative energy of the individual crystals to the vehicle approaches the fatigue or impact breaking strength of the materials used, snow erosion will be noticeable.

4.2 Sand Erosion

Sand or soil particle erosion has occasionally been reported on military aircraft flying at comparatively low altitudes over desert terrain. The phenomenon is ordinarily confined geographically, but might also be expected over "Dust Bowl" areas. Since the particles must be carried by air currents, a definite gradation of size distribution can be expected with altitude. The criteria for deciding what particle spectra to anticipate at altitude during a sandstorm is insufficiently not known, and the question is presumably unanswerable at this time.

As far as a missile is concerned, materials which can withstand up to a minute of sand blast with medium particles at missile speed will probably be satisfactory for radomes and leading edges.

4.3 Hail Erosion

The occurence of hail in dangerous quantities is sufficiently low as to pose no problem in the control of damage to aircraft and missiles. However, reports by NACA and the Military indicate that erosion and damage inflicted by hail when it does occur, is often sudden and severe.

Meteorological records are available for determining the sizes of hail which occur most frequently on the ground. For purposes of tests, these particles may be assumed to be airborne. Since an ice pellet, unlike a water drop, may be accelerated with an air blast, sample tests of the hail erosion-resistance in radomes and other materials are feasible.

4.4 Rain Erosion Simulation by Other Media

Conditions relating to Change of Erosion Medium.

A. Velocity Ratio

Since missile velocity increases with launch velocity, it becomes virtually impossible to simulate erosion for maximum-speed condition, due to the fact that the number of runs becomes prohibitively high. For speeds above M 3.5, an attractive possibility for reducing the cost of simulation is to use a higher-density liquid as the erosion agent.

The only high-density material which is a liquid at ordinary temperatures is mercury. If we stipulate that the relative kinetic energy contained by the drops shall be the same, and that whatever changes of state that take place shall be identical in kind and energy, then,

$$E_1 = E_2 \ \& \ \psi_1 = \psi_2 \tag{24}$$

where E is energy and ψ is the function of state of the two media.

For equal energy,

$$1/2\, m_{Hg}\ V_{Hg}^2 = 1/2\, m\ V_{H_2O}^2 \tag{25}$$

$$M_{Hg} = 13.546\ M_{H_2O}$$

$$V_{Hg} = \sqrt{\frac{\rho_{H_2O}}{\rho_{Hg}}}\ V_{H_2O} = 0.272\ V_{H_2O} \tag{26}$$

Where the test material is ceramic on plastic, mercury may be useable, but its action on metals and alloys should be investigated prior to test.

The curve in Figure 7 terminates about M 3.6 because of a change of state in mercury.

For any other pairs of media

$$V_1 = V_2 \sqrt{\frac{\rho_2}{\rho_1}} \qquad (27)$$

B. Changes of State

In order to be certain that the changes of state in the collision are the same, it is necessary to investigate the changes of state that may occur in ordinary rain erosion at high speeds. The first law of thermodynamics states that:

$$JQ = E \qquad (28)$$

Where J Joule's Equivalent
Q Quantity of Heat
E Energy of Impact

If the water is assumed to be liquid at the beginning of impact, and is allowed to achieve the vapor stage during impact, the Q term in equation

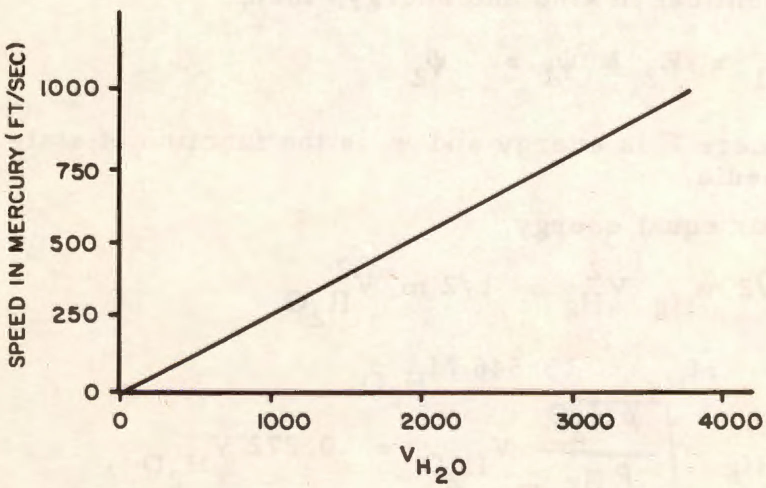

Figure 7 - Equivalent Test Speeds in Mercury (First Order Effects)

28 becomes: $$Q = Q_{liq.} + Q_L + Q_{v_{a_p}} \tag{29}$$

If the particles were ice crystals, or hail stones, Q terms for the solid state and latent heat of fusion would be added to those for the liquid and vapor states.

$$Q = Q_{sol} + Q_F + Q_{liq.} + Q_V + Q_{vap} \tag{30}$$

Terms 1, 3, & 5 are all of the form

$$Q = \int_{T_a}^{T_b} cdT \tag{31}$$

where c is the specific heat and T_a T_b are the initial and final temperatures achieved within a given state.

It is interesting to compare graphically the mercury and water changes of state. Figure 8 shows the permutation of water states for various initial temperatures.

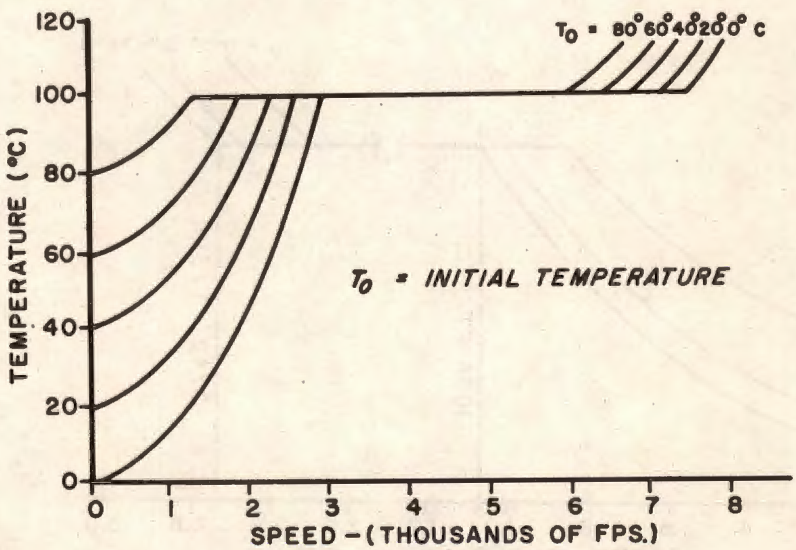

Figure 8 - Water Temperature After Impact

Sufficient energy is present to cause the water temperature to rise to the transition zone at a speed of about 3000 feet/sec no matter what the initial temperature was. If we avoid media conversion for transition zones, an upper limit near M 2.6 is imposed. Figure 9 shows the maximum range of liquid-to-vapor change in mercury. The low specific heat of mercury allows a rapid rise in temperature and the transition zone is reached by 1086 feet/sec.

Specific heat is in general a function of temperature, but in most instances may be taken as a constant throughout the temperature range of any given state, provided that additional states of freedom are not excited in the material. With this simplification and substitutuion from (30) into (29) we obtain an expression for the changes of state.

$$1/2\, mV^2 = J \left[(mc_{liq} (T_1 - T_o) + mq + mc_{vap} (T_2 - T_1) \right] \qquad (32)$$

$$\frac{V^2}{2J} = \Delta T_{liq}\, c_{liq} + q + \Delta T_{vap} c_{vap} \qquad (33)$$

q is the latent heat of fusion per unit mass. In using equation (33) it is necessary to take the right hand terms in sequence. That is, the

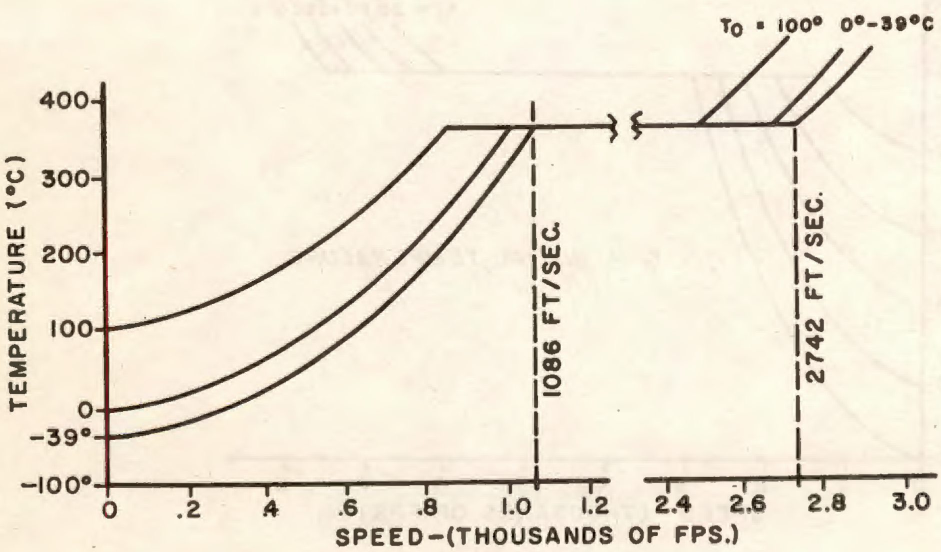

Figure 9 - Mercury Temperature After Impact

energy is first used to satisfy the initial term and the excess assigned to the second; then any excess of energy is then assigned to the last term. The final temperature may then be calculated. It is necessary to follow the same sequence as the physical-state transitions of the erosion medium. If a material is capable of additional degrees of freedom, additional terms reflecting the variation of c would be required.

If it is to be assumed that in both media, no part of the drop is vaporized before the whole mass, then the mercury is capable of simulating rain erosion up to the limit imposed by the water. Probably, however, this model is too simple to yield satisfactory solutions near the point where transition begins.

According to equations 27 and 33, the maximum equivalent speed for rain erosion which may be simulated up to the mercury transition zone is Mach 3.6 at sea level, but this assumes that all of the water remains liquid in the transition zone.

These considerations show that while the exact limits may not be prescribed at this time, the change of erosion media will not extend erosion measurement techniques much beyond Mach 3.

5. CONCLUSIONS

Current sled designs call for maximum speeds of about Mach 2. Assuming the restriction $K_m \approx K_s$, equation 22 can be used up to the transition zone of water (M 2.6). This means that erosion on a vehicle traveling M 2.5 can be simulated by using existing sled techniques. Since the condition of simulation does not hold for speed ratios greatly different than unity, special sleds capable of speeds of Mach 3, or above will be required if this manner of test is to be pursued for higher velocities. Such a sled might use a double or triple booster system and require 6 to 10 miles of track in order to get perhaps 2000 feet of useful rain field.

Generally, the current-type sleds will yield satisfactory results for missiles and aircraft in the speed range of M 1.5 to M 2.5. The time of flight at extreme speeds for aircraft must be prescribed in terms of radar limitations due to precipitation, fuel consumption, etc. in order to determine the number of sled runs required for a given simulation.

REFERENCES

1. D. Atlas Jour. Met. Vol 10 No. 6, Dec. 1953 pp 486-488
2. W. L. Dittmann, R. F. Holmes, E. T. Steeger et al. "A Study of Rain Erosion Testing Methods for Supersonic Speeds". WADC TR 53-173
3. Olive G. Engel, "Mechanism of Rain Erosion". WADC TR 53-192
4. J. S. Marshall and W. McK. Palmer. Jour. Met. Vol. 5, No. 4 Aug. 1948, pp 165-166.
5. McGill University. Stormy Weather Project, Report MW-7
6. N. E. Wahl, R. R. Lopp, et al. "A Study of the Rain Erosion of Plastics and Metals" WADC TR 53-185
7. G. P. Wetterburg, E. F. Pope & J. S. Murphy. "Raindrop Impingement on Various Bodies of Revolution at Sub and Supersonic Speeds". Vol I Proceedings of the Radome Symposium, page 1. Ohio State University June 1955.